ASIAN JOURNAL OF PHARMACEUTICAL AND CLINICAL RESEARCH

INNOVARE ACADEMIC SCIENCES
Knowledge to Innovation

Vol 18, Issue 10, 2025

Online - 2455-3891
Print - 0974-2441

Research Article

ITRACONAZOLE-LOADED NANOEMBEDDED MICROPARTICLES FOR INHALATION THERAPY IN LUNG INFECTIONS: DESIGN AND OPTIMIZATION

INDIRA MUZIB YALLMALLI*, SREEVIDYA PUVVALA

Department of Pharmaceutics, Institute of Pharmaceutical Technology, Sri Padmavati Mahila Visvavidyalayam, Tirupati, Andhra Pradesh, India.
***Corresponding author: Yallmalli Indira Muzib: Email: yindira1415@gmail.com**

Received: 20 June 2025, Revised and Accepted: 02 August 2025

ABSTRACT

Objective: To develop and optimize itraconazole (ICZ) nanoembedded microparticles (NMPs) for pulmonary delivery to enhance the treatment of aggressive pulmonary fungal infections, such as aspergillosis, in immunocompromised patients with chronic respiratory conditions by improving ICZ solubility, dissolution, and lung-specific drug delivery.

Methods: ICZ nanocrystals (INCs) were formulated using ultrasonic processing with poloxamer (PLX)-188 or Brij 58 as stabilizers to enhance solubility. Quality by design principles were applied to evaluate the effects of formulation and process variables on ICZ solubility and dissolution. Optimized INCs were lyophilized into NMPs using α-Lactose Monohydrate United States Pharmacopeia (USP) as a matrix, sifted to a particle size of <5 µm, and subjected to micromeritic and dissolution studies. The pharmacokinetic performance of NMPs was compared to commercially available oral ICZ formulations by assessing plasma drug concentrations.

Results: Optimized INCs, sonicated with PLX-188 at 50% amplitude for 15 min, achieved a particle size of 174.4 nm, solubility of 0.31 mg/mL, and a dissolution time of 22.97 min to reach 90% of the dose. NMPs exhibited suitable properties for inhalation, disintegrating in the secondary bronchi to release INCs that rapidly penetrated alveolar fluids. Compared to oral formulations, NMPs showed a faster tmax, higher Cmax, and increased plasma ICZ bioavailability at equivalent doses, with significantly higher drug concentrations in the lungs and sustained effective levels.

Conclusion: ICZ-loaded NMPs for pulmonary delivery offer a promising approach for treating pulmonary fungal infections, providing enhanced solubility, rapid dissolution, and superior lung-targeted drug delivery compared to oral formulations, potentially improving therapeutic outcomes in vulnerable populations.

Keywords: Itraconazole, Nanoembedded microparticles, Nanocrystallization, Quality by design, Inhalation, Pulmonary route, Aspergillosis.

 DOI: http://dx.doi.org/10.22159/ajpcr.2025v18i10.55673. Journal homepage: https://innovareacademics.in/journals/index.php/ajpcr

INTRODUCTION

Aspergillus fungus first infects the lungs [1], where it may spread to other organs. First-line treatments include antifungals, such as Itraconazole (ICZ) [2]. Even after systemic treatment, fatality rates are significant, and higher doses are impractical due to systemic toxicity. Therapeutically, a drug delivery system that delivers ICZ to the lungs is more effective. ICZ is water-insoluble and belongs to the BCS class II [3]. It involves in IV injection, oral solution, and delayed-release tablet form on the market. Poor and inconsistent bioavailability are drawbacks of the oral products [4]. Due to oral bioavailability issues, the inhalational route is more promising and necessary for improved therapeutic efficiency and patient compliance.

From the literature, it was found that amorphous solid dispersions (ASDs) of ICZ prepared by hot-melt extrusion with hydrophilic carrier Soluplus increased the solubility [5]. The ASDs were studied for several characterizations, including solubility and dissolution. The results demonstrated that both the solubility and dissolution were improved for the ASDs. Solid dispersions of ICZ using hydrophilic carriers, such as polyvinyl alcohol, Soluplus, and hydroxypropyl methyl cellulose by hot-melt extrusion were formulated and evaluated, and the results of the dissolution study showed that ICZ's dissolution was greatly increased from 1.5% in the case of pure drug to more than 80% for the solid dispersions after 2 h of dissolution [6]. Nanoprecipitation by solvent displacement was used with Tween 80 as the stabilizer for the formulation of a nanosuspension of ICZ to enhance the solubility [7]. The authors reported 96.8% dissolution for their best formulation against 34.5% for pure ICZ after 60 min. These results showed that hydrophilic carriers and surfactants can improve ICZ solubility and dissolution. However, none of these investigations examined pulmonary delivery of the compounded ICZ. Thus, ICZ administration through the lungs has great potential to be scientifically studied.

The pulmonary route provides advantages over the gastrointestinal tract, including high alveolar surface area, lack of first-pass metabolism, lower efflux transporter expression, and lower metabolic CYP450 enzymes [8-10]. In addition, the pulmonary route is ideal for local action against airborne diseases, including fungal aspergillosis and pulmonary disorders, such as asthma, bronchitis, and chronic obstructive pulmonary disorder [11]. In addition to these highly significant advantages, a few potential barriers to drug administration are also present in this route [12]. The major barriers among them are mucociliary clearance and pulmonary macrophages. The mucus lining in the airways captures and expels the dust particles and microorganisms. Hence, the drug particles may also be cleared before being absorbed systematically or before exerting their action locally. In Particular, the mucus present on the ciliary membrane is responsible for this clearance [13,14]. In addition, the endocytosis of the drug particles by the macrophages is another barrier [15-17]. Particles in the size range of 1–3 µm are more prone to phagocytosis in the lungs. This phagocytosis primarily depends on the size and surface properties of the administered drug particles, such as shape, surface charge, and adsorbed proteins [18-21]. A drug delivery system that can overcome these two barriers may be the best delivery system for either local or systemic action of any drug candidate.

The following hypothesis is formulated to improve therapeutic efficiency through pulmonary administration for local action on the basis of

disease etiology and ICZ solubility [22]. To improve ICZ solubility and dissolution, ICZ nanocrystals (INCs) were used. Poor aerodynamics make these nanoparticles inappropriate for pulmonary delivery. Thus, these INCs were embedded in a carrier to create nanoembedded microparticles (NMPs) of the ICZ without influencing dissolution. To achieve good aerodynamic qualities, NMPs were designed to be between 1.5 and 5 μm in size [23-25]. Thus, these NMPs may deposit in the lungs and dissolve promptly due to the high solubility of the carrier to avoid pulmonary endocytosis. The INCs released after solubilization of the carrier could easily diffuse into the alveolar network for dissolution and local activity.

A quality-by-design (QbD) strategy was used to prepare and optimize the INCs. Four different formulations and process variables were investigated to produce INCs with optimal solubility and dissolution. Later, the optimized INCs were lyophilized into a highly soluble lactose matrix. The lyophilized material was sieved to extract NMPs <5μm in size to obtain good aerodynamic properties while preserving the dissolution properties of INCs.

METHODS

Chemicals

ICZ was procured from Intas Pharmaceuticals Ltd., Poloxamer (PLX) 188, Brij 58, and α-Lactose monohydrate (particle size as D50 <5 μm) were acquired from Merck Ltd.

Development of INCs

QbD aspects

The development of INCs was envisaged using the nanocrystallization technique, with the application of ultrasonication. The Design Expert program facilitated the implementation of the QbD approach [26]. The quality target product profile was used to improve the solubility and dissolution rate of ICZ. Hence, the solubility (R1) and time for 90% dissolution (T90%) (R2) were taken as the response variables. On the basis of the literature and preliminary research, four distinct process and formulation factors were chosen to investigate their impact on the responses. The factors considered in the study were: A – sonication power (at amplitudes of 40%, 50%, and 60%), B – sonication time (at durations of 15, 20, and 25 min), C – stabilizer concentration (at concentrations of 0.25%, 0.5%, and 0.75% w/v), and D – stabilizer type (PLX 188 and Brij 58). The experimental design used to examine the effects of the factors on the responses was a central composite design (CCD). Table 1 displays the combinations of variables and their corresponding levels as per the CCD for the development of INCs.

Preparation of INCs

INCs were prepared by ultrasonication [27,28]. The INCs formulated with PLX-188 were designated as PINCs, whereas those formulated with Brij 58 were designated as BINCs. The stabilizer was dissolved in 20 mL of distilled water at the specified concentration. A quantity of 100 mg of ICZ was evenly distributed in the stabilizer solution mentioned previously. The dispersion was subjected to sonication using a Probe sonicator (Vibra Cell VCX 130, Sonics) at the appropriate amplitude for a defined duration. The stabilizer, its concentration, sonication amplitude, and time were selected according to the combinations specified in Table 1. Following sonication, the nanosuspension of the INCs was subjected to centrifugation at a relative centrifugal force of 5,800 g at 25°C for a duration of 100 min using an RM-12C centrifuge manufactured by Remi. The solid pellet of the INCs was subsequently obtained by separating it from the supernatant. The pellet was reconstituted in double-distilled water and dehydrated using lyophilization (followed by freezing, primary drying was at −40°C temperature and 1.3 millibar pressure, and secondary drying at 50°C) until the remaining moisture content is below 0.5%. The desiccated INCs were preserved in the identical vial for subsequent investigations.

Characterization studies of the INCs

Solubility

Pure ICZ and the INCs were studied by the equilibrium shake-flask method to determine the solubility [29,30]. In a stoppered test tube, 5 mL of water and extra ICZ/INCs were introduced. While on orbital shaker for 24 h, the test tube was tested for the need of ICZ/INCs addition. After 24 h of supersaturation, the mixture was filtered and spectrophotometrically examined. The solubility of only ICZ was also tested in 0.1N HCl, 0.1N NaOH, phosphate buffer with pH 3.4, 5.8, and 7.8 buffers.

Dissolution

INC's dissolution trials were done in 900 mL of 0.1 N HCl, the United States Food and Drug Administration (USFDA)-recommended medium [7] that was maintained at 37°C. A weight of 100 mg drug equivalent INCs from every formulation was taken for this test. The study lasted an hour with the Paddle device at 75 rpm. Dissolution samples were obtained periodically at 5, 10, 20, 30, 45, and 60 min and measured spectrophotometrically after suitable dilution. The data were kinetically processed with zero-order and first-order models, followed by calculating the dissolving rate constant (*k*) and T90%

Design validation and optimization

A sequential model sum of squares (SMSS) analysis was conducted for each response to determine the appropriate regression model between the factors and each response [26,31]. The proposed model subsequently underwent analysis of variance (ANOVA) testing to verify its validity and significance [32]. Ultimately, optimization was executed using the desirability functions approach. The desirability criteria were established to maximize solubility and minimize T90%. In addition, limitations were imposed on Factors A and B to minimize both the sonication power and time, taking into account the economic aspects of the procedure. Though the reduced sonication power and time are less important in the laboratory scale production, these are critical factors during scale-up for large-scale manufacturing.

Particle size and zeta potential

The optimized formulation of the INCs was subjected to dynamic light scattering analysis [33] with the Horiba SZ-100 instrument to measure the particle size and zeta potential of the optimized INCs. This study was conducted to verify the nanoscale dimensions of the INCs.

Preparation of NMPs

The INCs were embedded in lactose as the carrier. A solution of α-lactose monohydrate was prepared by dissolving 1 g in 5 mL of water in a glass vial, resulting in a saturated lactose solution. A quantity of 0.5 g of the optimized INCs was introduced into the lactose solution contained in the vial and stirred vigorously to create a uniform mixture. The dispersion was lyophilized (at −55°C temperature and 100 mTorr pressure) with LYB-5504 from Operon to generate a porous matrix of lactose with the INCs remaining embedded [34]. The porous matrix was removed to cause the structure to collapse. The sample was subsequently sieved through a Filson 5 μm stainless steel mesh to obtain a finely powdered substance known as NMPs.

Characterization of the NMPs

The NMPs that were obtained were analyzed by scanning electron microscopy (SEM) (TESCAN VEGA3) [35-37], and micromeritic properties, such as the mass median aerodynamic diameter (MMAD) [38], were analyzed by following established protocols. In addition, the NMPs underwent dissolution experiments as described in Section 2.3.2 to examine any alterations in the dissolution rate of the INCs caused by the lyophilization procedure.

Differential scanning calorimetry (DSC)

The INCs and the NMPs were subjected to a DSC (NEXTA, HITACHI) study to investigate any changes in the physical state of the drug after

converting the nanocrystals were converted into NMPs. At a heating rate of 10°C/min, thermal analysis in a nitrogen atmosphere was performed at a temperature range of 50–300°C.

The NMPs were also characterized for the following micromeritic properties:

Bulk density

Two grams of precisely measured NMPs were inserted into a 10 mL measuring cylinder. The NMPs volume was measured without disrupting the cylinder, and the bulk density was determined using the following formula.

$$\text{Bulk density} = \frac{\text{Weight of sample}}{\text{Volume of sample}}$$

Tapped density

The above measuring cylinder containing 2 g of the NMPs was dropped on a hard wooden surface from a 1-inch height at 2-s intervals for 100 times. From the final volume, the tapped density was calculated by the following equation

$$\text{Tapped density} = \frac{\text{Weight of sample}}{\text{Tapped Volume of sample}}$$

Carr's index (%)

This is an indication of the compressibility of a powder. It is calculated by the formula.

$$\text{Carr's Index}(\%) = \frac{\text{Tapped density} - \text{Bulk density}}{\text{Tapped density}} \times 100$$

Hausner's ratio

This is an indicator of the flowability of a powder. It is calculated by the formula:

$$\text{Hausener's ratio} = \frac{\text{Tapped density}}{\text{Bulk density}} \times 100$$

Angle of repose (θ)

The funnel was positioned such that the stem of the funnel was elevated 2.5 cm above the flat surface. The NMP powder was discharged from the funnel, causing the pile to reach the top of the funnel. The diameter of the pile was estimated by delineating a boundary along the perimeter of the pile and calculating the mean of three diameters. The angle of repose is calculated by using this formula:

$$\theta = \tan^{-1} h/r$$

where, θ is the angle of repose, h is the height of the pile, and r is the radius of the pile.

MMAD

MMAD was calculated using the below formula

$$\text{MMAD} = \text{Size x}\sqrt{\text{true density}}$$

True density of the NMPs was determined by the standard procedure of the mercury displacement method using a pycnometer.

***In vivo* pharmacokinetic studies**

The protocol for the *in vivo* study was examined and approved at Hindu College of Pharmacy, Guntur, and given the number IAEC-HCOP/2023/08. Male Sprague-Dawley rats of 7–9 months old with a weight ranging from 200 to 250 g were taken as the experimental animals. For 2 weeks, the animals were kept at 25±0.5°C and 50±5% relative humidity with 12-h light/dark cycles. The animals had unrestricted access to food and water during this period. Twelve hours before the investigation, the animals were kept in a fasting state.

A total of 36 animals were taken and divided into 3 groups equally and named as G1: Control (administered with potable water at 5 mL/kg body weight), G2: Reference product (Marketed oral solution, Itratuf Oral Solution 10 mg/mL by Alkem Lab Ltd.), and G3: Test treatment (NMPs formulation). The dose for both the Reference and the test product was at 40 mg/kg body weight [39]. The animals in G2 were administered with the dose equivalent amount of the reference product through the oral route using an oral gavage. On the other hand, the animals in the G3 were administered with the test formulation of NMPs (75 mg of the NMPs contain 10 mg of INCs for a 250 g of rat) using an in-house developed hand-operated inhalation device as described by Kaur *et al.* [40]. A hole was drilled in the apex of a centrifuge tube for inserting a flexible air input tube. The tube wall had another hole for the delivery port, which could fit a rat's muzzle. A pipette bulb was fixed on the flexible tubing and its activation allowed turbulent air to fluidize the powder for inhalation by the rats. At specified time intervals 0.5, 1.0, 1.5, 2.0, 3.0, 6.0, 12.0, 18.0, and 24.0 h, blood samples were collected from retro-orbital into heparinized tubes and centrifuged to collect plasma. Blood samples were collected only from three animals from each group at every time point. Furthermore, one animal from each group was euthanized at every time point and the lung tissue was isolated and checked for its weight. The tissue was added into phosphate buffer saline solution and homogenized to a fine dispersion. Both the plasma samples and the homogenized tissue samples were subjected to a liquid-liquid extraction method using methanol as reported by Compas *et al.* [41]. Then the extracted samples were subjected to chromatographic analysis to quantify the ICZ levels. The obtained data were analyzed through a non-compartmental model using the PK Solver [42] to calculate the pharmacokinetic parameters of ICZ from both the products in both blood and lungs tissue. For each pharmacokinetics property, the significance in the difference in the results between both the products was tested by a t-test. For this purpose, two sample t-test assuming unequal variances was adopted at α level of 0.05.

Stability studies

Accelerated stability testing was executed on the optimized NMPs of both the drugs according to the ICH conditions as per the guidelines of Q1A(R2). The NMPs were packed in glass vials and were stored at 40±2°C temperature and 75±5% RH humidity for 6 months. At intermediate time intervals of 3 and 6 months, samples were taken and analyzed visually for any observable change as well as for the drug content and drug release studies.

RESULTS AND DISCUSSION

The solubility of pure ICZ in water was found to be below 0.003 mg/mL. As the lower limit of the linearity was 3 µg/mL by the developed spectroscopy method in our study, any solubility below this could not be accurately determined. Its solubility in 0.1N HCl and in phosphate buffer pH 3.4 were found to be 0.048 and 0.016 mg/mL, respectively. Whereas its solubility in phosphate buffers pH 5.8, pH 7.8, and in 0.1N HCl were found to be below 0.003 mg/mL. Its maximum solubility in 0.1N HCl could be due to its alkaline nature. The results of the solubility analysis of the INCs are presented in Table 1.

The INCs were nanocrystallized through ultrasonication. Sonication can reduce the particle size to the nanoscale. Extreme particle size reduction can produce static charge and nanoparticle aggregation. This agglomeration reduces the effective solid surface area, thereby reducing the increase in solubility. Hence, a stabilizer was added to the sonication medium to prevent agglomeration. The stabilizers used were PLX 188 and Brij 58 [43,44]. Both are hydrophilic non-ionic surfactants that can adsorb on ICZ particles during size reduction. Thus, these materials reduce the interfacial tension, free energy, and agglomeration [45], which ultimately improves the solubility and dissolution. The solubility

Table 1: Central composite design - suggested combinations of the factors with levels indicating various formulations of INCs

Formulation code	Levels of the factors				R1: Solubility (mg/mL) mean±SD (n=3)	R2: T90% (min.) Mean±SD (n=3)
	A: Sonication power	B: Sonication time	C: Stabilizer conc.	D: Stabilizer type		
PINC1	50	20	0.08	PLX-188	0.03±0.01	37.5±3.2
PINC2	40	15	0.25	PLX-188	0.02±0.01	40.9±2.4
PINC3	60	15	0.25	PLX-188	0.10±0.04	32.8±1.6
PINC4	40	25	0.25	PLX-188	0.07±0.02	40.1±1.9
PINC5	60	25	0.25	PLX-188	0.16±0.05	27.9±2.5
PINC6	50	11.59	0.5	PLX-188	0.21±0.03	31.6±3.2
PINC7	33.18	20	0.5	PLX-188	0.19±0.06	32.7±1.4
PINC8	50	20	0.5	PLX-188	0.23±0.07	29.2±1.7
PINC9	66.82	20	0.5	PLX-188	0.33±0.04	20.4±2.1
PINC10	50	28.41	0.5	PLX-188	0.36±0.08	23.5±1.6
PINC11	40	15	0.75	PLX-188	0.29±0.05	27.3±1.9
PINC12	60	15	0.75	PLX-188	0.31±0.02	21.9±3.4
PINC13	40	25	0.75	PLX-188	0.28±0.03	22.8±2.8
PINC14	60	25	0.75	PLX-188	0.35±0.01	20.3±2.5
PINC15	50	20	0.92	PLX-188	0.31±0.07	24.9±1.3
BINC1	50	20	0.08	Brij 58	0.02±0.01	45.2±1.8
BINC2	40	15	0.25	Brij 58	0.01±0.01	47.3±1.1
BINC3	60	15	0.25	Brij 58	0.04±0.01	44.7±2.9
BINC4	40	25	0.25	Brij 58	0.05±0.01	45.9±3.4
BINC5	60	25	0.25	Brij 58	0.12±0.03	38.5±2.7
BINC6	50	11.59	0.5	Brij 58	0.15±0.04	35.4±1.8
BINC7	33.18	20	0.5	Brij 58	0.13±0.02	36.2±4.2
BINC8	50	20	0.5	Brij 58	0.20±0.07	33.1±1.6
BINC9	66.82	20	0.5	Brij 58	0.24±0.05	31.8±2.4
BINC10	50	28.41	0.5	Brij 58	0.21±0.02	30.9±1.7
BINC11	40	15	0.75	Brij 58	0.17±0.01	33.6±3.1
BINC12	60	15	0.75	Brij 58	0.26±0.05	25.4±2.5
BINC13	40	25	0.75	Brij 58	0.23±0.04	29.7±2.2
BINC14	60	25	0.75	Brij 58	0.31±0.03	24.2±1.3
BINC15	50	20	0.92	Brij 58	0.29±0.06	24.9±1.9

PINC: Polaxomer-188 itraconazole nanocrystals, BINC: Brij-58 itraconazole nanocrystals, PLX: Poloxamer, SD: Standard deviation

and dissolution rate of the prepared INCs were investigated to confirm these assumptions. Table 1 shows the solubility and T90% data.

Experimental design validation

The findings of the SMSS analysis (shown in Table 2) indicated that the factors had an impact on both responses that was linear. The linear models for the solubility and the T90% were determined to be significant at $p<0.05$, according to the findings of the ANOVA test [46] which are displayed in Table 3. Furthermore, each of the four factors significantly affected the solubility and the T90% at $p<0.05$. In addition to the ANOVA test, the predicted versus actual plots for both responses are shown in Fig. 1. These plots both responses demonstrated that all of the data points were evenly distributed around the line 45°. This discovery suggested that no transformation of the data is required before proceeding with DoE analysis and optimization.

DoE analysis of the responses

Fig. 2a-d illustrates the impacts of various factors on the solubility of INCs. An increase in sonication power, as measured by the amplitude (Factor A) and duration of sonication (Factor B), lead to an increase in solubility. The application of high-amplitude sonication increases the energy input into the dispersion, leading to a more significant reduction in the size of the INCs. Increasing the duration of sonication also results in more energy being applied to the dispersion, potentially leading to a reduction in particle size [47,48]. Reducing the particle size of the INCs may lead to an increase in their solubility. The solubility was enhanced by an increasing in the concentration of the stabilizer (Factor C). Increased concentrations of the surfactants, PLX-188 and Brij 54, result in increased adsorption of these molecules onto the surface of the INCs. This leads to the formation of steric barriers, which in turn reduce aggregation and results in reduced particle size and increased surface area. In addition, the adsorption of larger quantities of these hydrophilic surfactants can increase the hydrophilicity of the surface of solid particles. Gigliobianco *et al.* [49], and Gulsun *et al.* [50] reported similar impacts of surfactants on the surface characteristics and solubility of the poorly soluble drugs. Therefore, INCs that have a larger surface area and a greater quantity of adsorbed surfactants lead to an increased solubility of ICZ. The acquired results strongly correlate with the findings reported by dos Dos Santos *et al.* [51]. The solubility of ICZ was greatly affected by the type of stabilizer (Factor D). Compared with Brij 58, PLX-188 showed a greater ability to enhance the solubility of ICZ. This can be explained by the higher hydrophilic-lipophilic balance (HLB) value of PLX-188, which is 29, than the HLB value of Brij 58, which is 16. PLX-188, with a higher HLB, is a more hydrophilic. Consequently, it significantly enhances the solubility of ICZ to a greater degree than Brij 58 does. A similar effect of the HLB of the surfactant on the solubility of Ketorolac was observed, as reported by Smail *et al.* [52].

Table 2: Sequential model sum of squares analysis results for the response solubility and T90%

Source	Model p value	Adjusted R^2	Predicted R^2	Inference
For solubility				
Design model	0.0001	0.8863	−1.0415	
Linear	<0.0001	0.8816	0.8526	Suggested
2FI	0.9762	0.8530	0.7769	
Quadratic	0.0344	0.8967	0.8062	Suggested
Cubic	0.8310	0.8553	−1.3805	
For T90%				
Design model	0.0001	0.8836	−0.0542	
Linear	<0.0001	0.8919	0.8644	Suggested
2FI	0.3684	0.8958	0.8175	
Quadratic	0.3120	0.9004	0.8076	
Cubic	0.2185	0.9368	−0.0120	Aliased

Table 3: Analysis of variance test results of quadratic models for the responses solubility and T90%

Source	Sum of squares	Degrees of freedom	Mean square	F-value	p-value	Inference
For solubility						
Model	0.3131	4	0.0783	55.00	<0.0001	Significant
A-sonication power	0.0331	1	0.0331	23.24	<0.0001	Significant
B-sonication time	0.0191	1	0.0191	13.45	0.0012	Significant
C-stabilizer concentration	0.2390	1	0.2390	167.93	<0.0001	Significant
D-stabilizer type	0.0219	1	0.0219	15.37	0.0006	Significant
Residual	0.0356	25	0.0014			
Correlation total	0.3487	29				
For T90%						
Model	1635.13	4	408.78	60.79	<0.0001	Significant
A-sonication power	234.23	1	234.23	34.83	<0.0001	Significant
B-sonication time	76.43	1	76.43	11.37	0.0024	Significant
C-stabilizer concentration	1036.17	1	1036.17	154.09	<0.0001	Significant
D-stabilizer type	288.30	1	288.30	42.87	<0.0001	Significant
Residual	168.11	25	6.72			
Correlation total	1803.25	29				

A p<0.05 indicates the model terms are significant

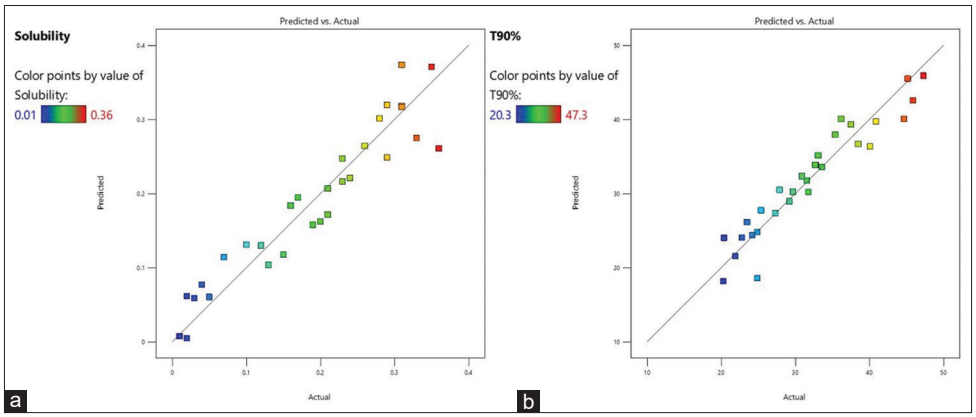

Fig. 1: Predicted versus actual plots for the responses (a) solubility and (b) T90%

Fig. 3a-d depict the impacts of all the factors on the T90% of the INCs. Increasing the levels of the factors, A and B results in a decrease in T90%, indicating an increase in the dissolution rate. The solubility of ICZ was positively influenced by these two factors. Furthermore, subjecting the dispersion to sonication at a greater power for more time can also lead to a reduction in particle size [51]. The enhanced solubility and reduced particle size of the ICZ may lead to accelerated dissolution from the INCs, resulting in a drop in the T90%. By increasing the level of the Factor C, the T90% decreased. The solubility of ICZ was significantly increased with increasing concentrations of the surfactants PLX-188 and Brij 54. Moreover, surfactants tend to reduce the interfacial tension and enhance wetting [53]. These combined properties could lead to a quick disintegration with a lower T90%. The T90% of the ICZ was greatly influenced by the Factor D. Compared Brij 58, PLX-188 exhibited a greater rise in dissolution rate and greater decrease in T90% when the two stabilizers were compared. PLXs have the capacity to reduce the occurrence of solid steric stabilization precipitation. This property in addition to besides the higher hydrophilicity of PLX-188 might cause rapid dissolution of the PINCs compared with BINCs. These results were in agreement with those reported by Dos Santos *et al.* [51].

Optimization

The optimization results were extracted from the software and presented as an overlay plot, as depicted in Fig. 4. The minimum threshold for achieving optimal solubility was established at 0.25 mg/mL, indicating that the solubility must exceed 0.25 mg/mL. The maximum threshold for reducing the T90% was established at 30 min, meaning that the T90% must be <30 min. In addition, the Factors A and B were set to a minimum so as to make the process more economical. On the basis of these criteria, the overlay plot that was obtained showed a region with a yellow color, which is referred to as the design space.

The software designated a specific combination of parameters within the design space and projected their values for both responses, as shown in Table 4. New INCs were prepared at the recommended levels of the factors, that is, INCs were prepared with 0.75% w/w of PLX-188 at amplitude of 50% for 15 min. These properties were subsequently examined for their solubility and dissolution rate. The solubility of these INCs was determined to be 0.31 mg/mL, and the T90% was measured to be 22.97 min. The responses of the optimized formulation were determined to fall within the 95% confidence intervals of the projected values (Table 4). Hence, this formulation of the INCs was taken as the optimized formulation for further characterization and development. Though the reduced sonication power and time are less important in the laboratory scale production, these are more critical factors during scale-up for large-scale manufacturing. Hence, this optimized formulation at lower sonication conditions can be better considerable for scale-up studies.

Particle size and zeta potential

The optimized INCs were additionally analyzed for particle size and zeta potential. The empirical findings are depicted in Fig. 5a and b. The analysis revealed that the particle size was 174.38 nm, with a polydispersity index of 0.284. In addition, the zeta potential was determined to be −9.43 mV. The observed values of particle size and zeta potential indicate that the INCs can readily spread into the alveolar region without being significantly impacted by phagocytosis [54,55]. However, these particles at the nanoscale have suboptimal aerodynamic characteristics and are unsuitable for direct administration through breathing [56]. Hence, their size needs to be increased, without altering

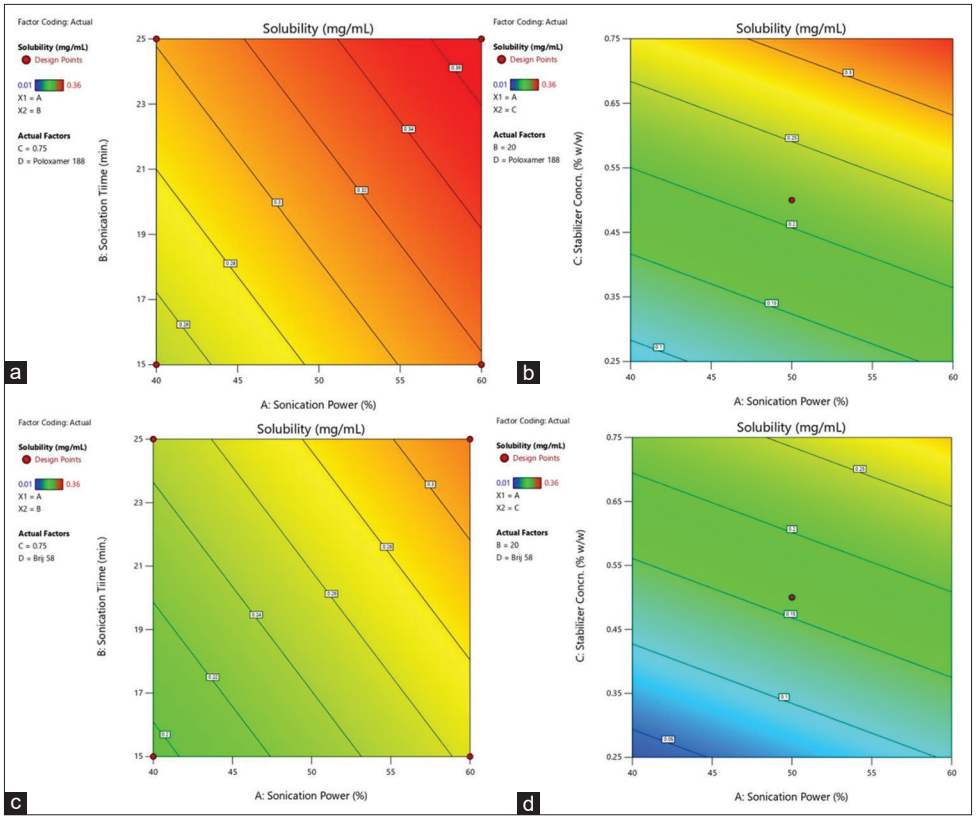

Fig. 2: Displaying influences of the factors (a) A and B, and (b) A and C on R1 in the case of poloxamer-188; influences of the factors (c) A and B, and (d) A and C on R1 in the case of Brij 54

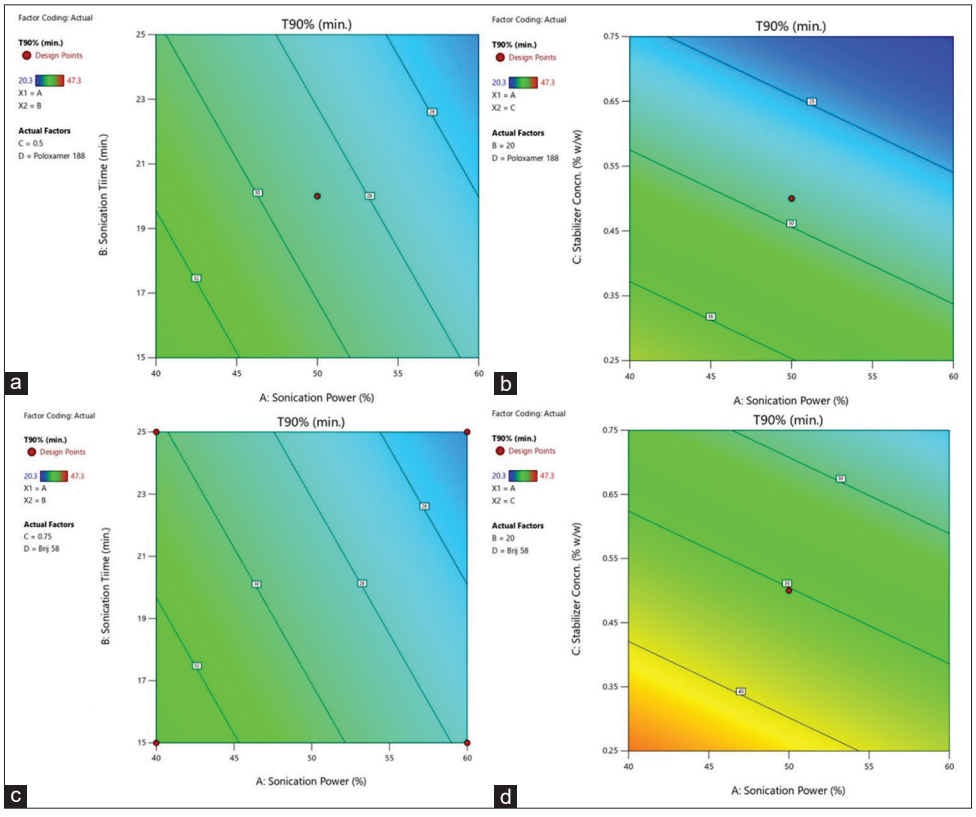

Fig. 3: Displaying influences of the factors (a) A and B, and (b) A and C on R2 in the case of poloxamer-188; influences of the factors (c) A and B, and (d) A and C on R2 in the case of Brij 54

Table 4: Optimized INCs combined with the predicted and the observed values of the responses

Factors combination	Responses	Predicted values	95% CI low	95% CI high	Observed values
A: Sonication power. (50% amplitude) B: Sonication time (15 min.) C: Stabilizer concentration (0.75% w/w) D: Type of stabilizer (poloxamer-188)	R1: Solubility (mg/mL) R2: T90% (min.)	C0.28 24.40	0.25 22.44	0.31 26.43	0.31 22.97

95% CI: Confidence interval, INC: Itraconazole nanocrystal

Table 5: Results of the micromeritic properties of the NMPs

S. No.	Property	Method	Observed results*
1	Mean particle size (µm)	Optical microscopy	4.71±0.56
2	True density (g/cc)	Liquid displacement	1.48±0.32
3	Aerodynamic diameter (µm)	Size×(True density) $^{1/2}$	5.73±0.51
4	Bulk density (g/cc)	Bulk density apparatus	0.61±0.04
5	Tapped density (g/cc)	Bulk density apparatus	0.67±0.06
6	Angle of repose (°)	Fixed funnel method	15.39±1.17
7	Carr's index (%)	Bulk density apparatus	8.82±2.20
8	Hausner's ratio	Bulk density apparatus	1.10±0.03

*Presented as Mean±standard deviation for n=3

the solubility and dissolution rate, to achieve enhanced aerodynamic qualities that are suitable for inhalation.

Development and characterization of NMPs

Compared with pure ICZ, INCs show substantial increases in both solubility and dissolution, resulting in the rapid dissolution of ICZ to produce local action at the administration site. However, these traits alone are inadequate for the administration of INCs through inhalation. To achieve inhalational administration with desirable aerodynamic features, an increase in the size of these INCs to a maximum size of 5 µm is necessary. Therefore, in this study, the INCs were incorporated into a safer inhalational grade lactose [57] matrix to create the NMPs. These NMPs underwent multiple characterization investigations to verify their enhanced aerodynamic properties while maintaining their dissolution characteristics. The NMPs were analyzed for their micromeritic features, surface morphology through SEM, and DSC investigations. In addition, the NMPs underwent dissolution experiments to examine any alterations in the dissolution rate resulting from the lyophilization process. The micromeritic characteristics are displayed in Table 5. As per the European pharmacopoeia, the powders with the Hausner's ratio of more than 1.25 and Carr's index of more than 25 are poor-flowing powders. However, the observed Carr's index and Hausner's ratio values of the NMPs were well below these ranges and thus indicate good flowability. The average particle size obtained was 4.71 µm. The aerodynamic diameter was obtained as 5.73 µm. The dimensions of the NMPs make them well-suited for administration through inhalation as the optimal range is 1–5 µm [23-35]. When these particles of a specific size range are breathed in, they can easily dissolve in the secondary bronchi, resulting in the formation of INCs. These INCs have the ability to quickly move into the fluids in the alveoli for immediate local effects. The NMPs possess favorable capabilities for inhalation as dry powder, as evidenced by their aerodynamic diameter and other flow characteristics.

The NMPs obtained following lyophilization and sieving were analyzed through SEM to examine their surface appearance. The resulting image, shown in Fig. 6, demonstrated that the NMPs were nearly square-shaped and had a consistent texture. This can be attributed to the lyophilization and sieving procedures. Despite not being perfectly spherical, the NMPs demonstrated favorable micromeritic characteristics (as indicated in Table 5) that are essential for a powder intended for dry inhalation. The DSC spectra of the INCs, depicted in Fig. 7, displayed a distinct and intense endothermic peak at a temperature of 170.06°C. The peak position corresponds to the melting point temperature of crystalline

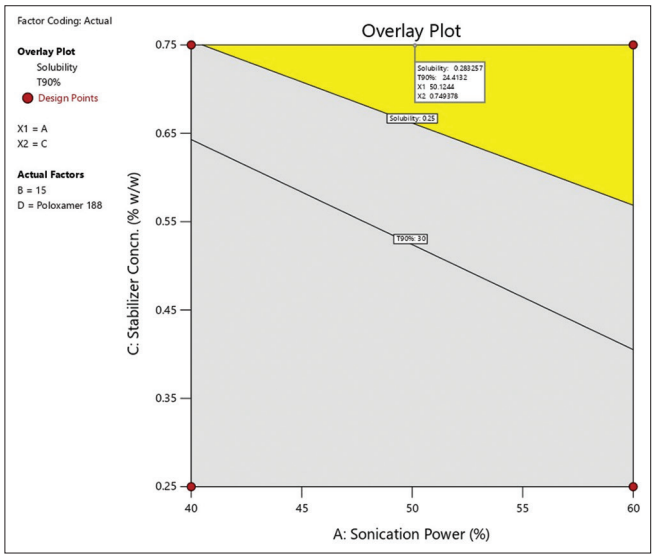

Fig. 4: Illustration of the design space resulting from optimization

ICZ. Following the incorporation of these nanocrystals into lactose within the NMPs, a subsequent DSC study was performed. This spectrum exhibited a distinct endothermic peak at a temperature of 169.28°C. This observation demonstrated that ICZ remained in its crystalline structure and that the procedure of embedding through lyophilization, aimed at increasing its size, did not alter the crystalline nature of the medication. This observation verifies that the solubility and dissolving properties of the INCs will remain unchanged, while providing aerodynamic benefits owing to their larger size when transformed into NMPs. Fig. 8 displays the dissolution profiles of the pure ICZ, the optimized INCs, and the NMPs. Compared with that of the pure drug the dissolution rate of the ICZ significantly increased when the INCs were prepared. The T90% of the pure ICZ was found to be 192.3 min and the T90% of the ICZ from the optimized INCs was determined to be 24.6 min, which was a 7.8-fold increase. The aforementioned INCs were subsequently incorporated within the lactose matrix, to obtain micron-sized NMPs. The dissolution profile of the ICZ from these NMPs closely resembled that of the ICZ from the INCs, with a T90% value of 25.8 min. The observation for the results of the dissolution test indicated that the dissolution of ICZ remained nearly unchanged and did not show major alterations upon the conversion of the INCs into NMPs. These obtained results were strongly correlated with those reported by Li *et al.* [58].

***In vivo* pharmacokinetics studies**

After administration of the assigned formulations, blood samples were taken at specified time intervals. One animal at every time point was euthanized and the lungs tissue was collected. The weight of the lungs collected was checked, followed by homogenization. These blood and the homogenated lungs samples were subjected HPLC to quantify the ICZ concentration.

First the comparison between the plasma drug levels from both the formulations was made. The comparative plasma drug levels plot is illustrated in Fig. 9. This data were subjected to non-compartmental analysis using PK Solver to obtain various pharmacokinetic parameters, namely, maximum plasma concentration (C_{max}), time for

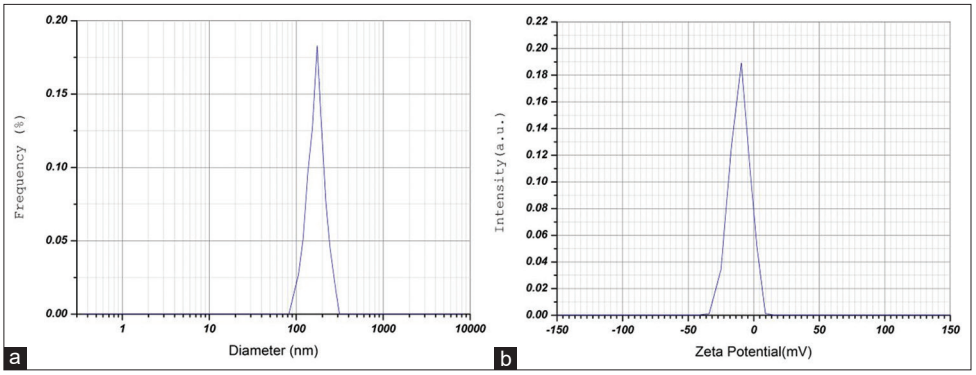

Fig. 5: Depiction of (a) particle size distribution and (b) zeta potential curves of the optimized itraconazole nanocrystals

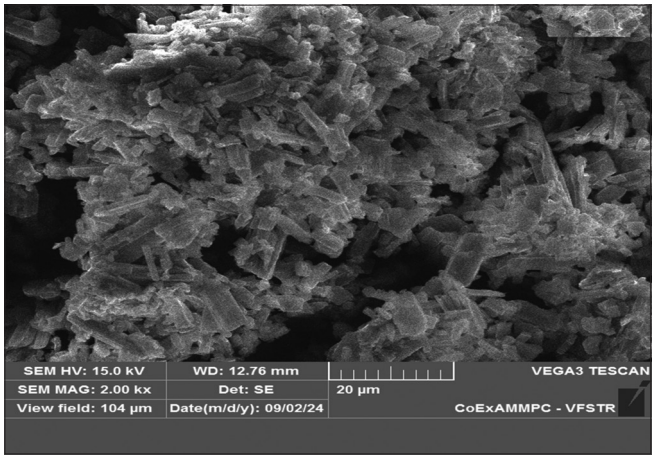

Fig. 6: Illustration of the surface morphology of the nanoembedded microparticles

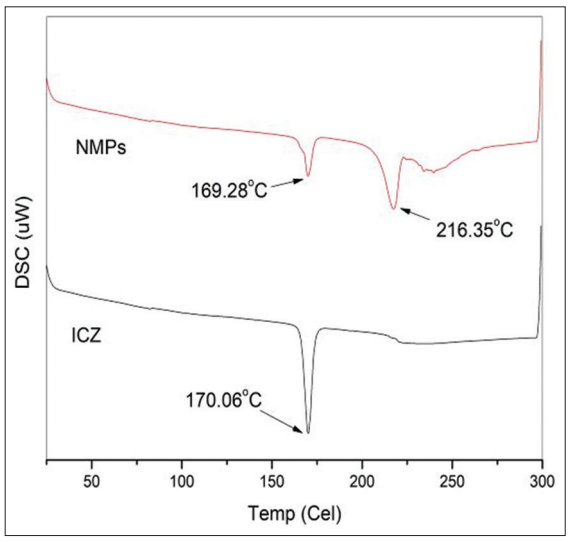

Fig. 7: Differential scanning calorimetry thermograms of itraconazole, itraconazole nanocrystals, and nanoembedded microparticles

C_{max} (T_{max}), area under the curve (AUC_{0-t} and $AUC_{0-\infty}$), elimination half-life ($t_{1/2}$), volume of distribution per bioavailable fraction (V_d/F) and clearance per bioavailable fraction (Cl/F). The obtained results are shown in Table 6. Table t-value for two-tail t-test for the data is 2.77. The calculated t-values and their corresponding *p* values are shown in Table 6.

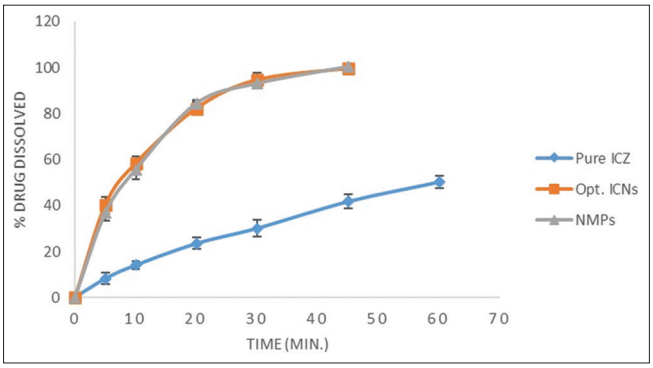

Fig. 8: Comparison of dissolution profiles of pure itraconazole, itraconazole nanocrystals and nanoembedded microparticles

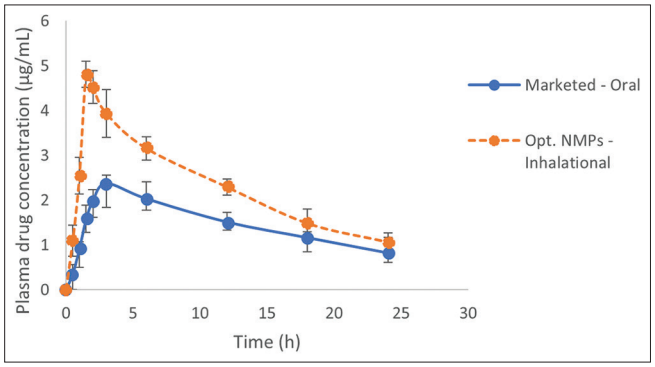

Fig. 9: Comparison between drug levels in plasma from the marketed itraconazole formulation given through oral route and the optimized nanoembedded microparticles given through inhalational route

The results of the t-test inferred those significant differences at $p<0.05$, between both the products were observed with all the bioavailability indicating parameters, namely, T_{max}, C_{max}, AUC_{0-t}, $AUC_{0-\infty}$ and V_d/F. However, there were not significant differences were observed with $t_{1/2}$ and Cl/F. A difference in formulation can alter dissolution and/or permeability and hence the bioavailability can be changed and hence the bioavailability indicating parameters were found significantly different for both the formulations. In addition, a difference in route of administration can alter the extent of distribution and hence the obtained Vd/F values were significantly different from both the route of administration for both the formulations. Whereas, elimination from plasma is same for a same drug irrespective of differences in formulations and hence no significant difference was observed with both the formulations. The T_{max} was found to be rapid and the C_{max} was found to be higher from the NMPs when compared to oral marketed product. These results illustrated that the

Table 6: Pharmacokinetic parameters of itraconazole from the test and reference products from the plasma drug concentration data

Pharmacokinetic parameter	Obtained values as mean±standard deviation for n=3		t-test statistics#	
	Marketed product (Oral)	Optimized nanoembedded microparticles (Inhalational)	Calculated t-value	p-value*
T_{max} (h)	3.00	1.50	12.39	0.0011
C_{max} (µg/mL)	2.37±0.19	4.81±0.29	12.19	0.0012
AUC_{0-t} (h. µg/mL)	35.26±1.83	55.44±2.72	10.66	0.0004
$AUC_{0-\infty}$ (h. µg/mL)	51.76±2.04	72.43±3.16	9.52	0.0025
$t_{1/2}$ (h)	13.95±1.42	11.10±1.57	2.33	0.0801
Vd/F (L/kg)	15.56±1.92	8.85±0.74	5.65	0.0109
Cl/F (L/h)	0.77±0.15	0.55±0.12	1.98	0.1183

*p<0.05 indicates significant differences

Table 7: Pharmacokinetic parameters of itraconazole from the test and reference products from the lungs drug concentration data

Pharmacokinetic parameter	Obtained values as mean±standard deviation for n=3		t-test statistics	
	Marketed product (oral)	Optimized nanoembedded microparticles (inhalational)	Calculated t-value	p-value*
AUC_{0-t} (h. µg/mL)	43.70±3.26	3081.24±131.52	39.99	0.0006
$AUC_{0-\infty}$ (h. µg/mL)	63.01±4.69	3144.97±139.08	38.36	0.0007
$t_{1/2}$ (h)	14.86±1.42	12.55±1.34	2.05	0.1098
V_d/F (L/kg)	13.61±1.24	0.23±0.05	18.67	0.0028
Cl/F (L/h)	0.63±0.08	0.01±0.002	13.42	0.0055

*p<0.05 indicates significant differences

Table 8: Results of characteristic properties of the nanoembedded microparticles of itraconazole during and at the end of accelerated stability studies

S. No.	Characteristic property	Observed value* at		
		0 months	3 months	6 months
1	Physical appearance	Free-flowing white powder	No observable changes	No observable changes
2	Drug content (%)	98.57±2.03	97.49±1.54	98.01±1.93
3	Angle of repose	15.39±1.17	13.56±2.32	16.22±1.58
4	Particle size (µm)	4.71±0.56	4.92±0.31	4.86±0.25
5	Time for 90% dissolution (T90%) (min.)	25.80±1.92	23.42±0.73	26.53±1.46

*The values are expressed as average±standard deviation for n=3

bioavailability of ICZ from plasma data was significantly enhanced upon given through inhalational route in the form of NMP when compared to the marketed oral solution at same dose. An increase in bioavailability by 39.9% (as expressed using $AUC_{0-\infty}$) was observed with the optimized NPMs. This could be attributed to the enhanced solubility of ICZ in the NMPs. In a previous study reported by Shin *et al.* [59] the bioavailability of ICZ from oral and IV routes were investigated. The authors Shin *et al*. had an obvious observation that ICZ had lesser bioavailability from oral route in comparison to IV route. These authors reported that the cause for this lesser bioavailability could be the first-pass metabolism of ICZ. In the present investigation also, ICZ even in the form of oral solution exhibited lesser bioavailability from oral route when compared to inhalational route. Hence, this could be justified to be due to the first-pass metabolism from oral route. In addition, the V_d/F was significantly decreased in case of NMPs which signified that more confinement of the drug in lungs when given through inhalational route. This observation signified that greater availability of drug in the lungs from the NMPs given through inhalational route.

The lungs drug levels from both the test and reference products, as expressed in µg/g (µg of drug per one g of lung tissue), are illustrated in Fig. 10. The pharmacokinetic parameters calculated form the lungs drug levels by non-compartmental analysis are presented in Table 7. The table t-value for a two-tail t-test for the data is 2.77. The calculated t-values and the corresponding p-values are presented in Table 7.

The findings of the t-test inferred those significant differences at p<0.05, between both the products were observed with AUC_{0-t}, $AUC_{0-\infty}$ and Cl/F. The Initial drug level from the inhalational NMPs was observed to be many times higher when compared to those from the oral marketed product. This could be attributed to the direct delivery of ICZ by the NMPs into lungs. The concentration of ICZ from the NMPs at 0.5 h was found to be 3726.14 µg/g. Weight of the lung tissue collected was found to be 1.5 g. This means a total of 5589.21 µg or 5.59 mg of ICZ was deposited in the lungs. The administered dose was at 10 mg per an animal of weight 250 mg. Hence, the success rate of pulmonary delivery of ICZ from the NMPs was found to be 55.9%. The lungs $AUC_{0-\infty}$ of ICZ from the inhalational route was found to be 3144.97 h. µg/

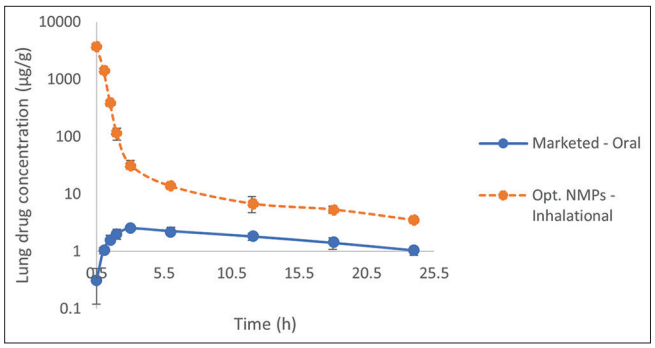

Fig. 10: Comparison between drug levels in lungs from the marketed ICZ formulation given through oral route and the optimized NMPs given through inhalational route

mL, which was 49.9 time more when compared to that from the oral marketed product which was 63.01 h.µg/mL. Buil *et al.* [60] reported minimum inhibitory concentrations of ICZ along with posaconazole and voriconazole in wild-type and acid-resistant Aspergillus fungi species. For ICZ, the Minimum Inhibitory Concentration (MIC) was reported to be >1 µg/mL. Hence, by considering this 1 µg/mL as the MIC, effective drug levels in the lungs were maintained for longer time form the inhalational NMPs when compared to the oral marketed product which was supported by the observed clearance values. Further, significantly lesser V_d/F and lesser Cl/F for NMPs from the lungs data demonstrated localization of higher drug concentration in the lungs for extended time period. These findings altogether demonstrated that the NMPs were highly effective in delivering significantly higher amounts of drug into lungs and also could maintain effective drug levels in the lungs for longer time when compared to the conventional oral route. Hence, the formulated NMPs were found to be capable of delivering the loaded drug into lungs. Further, pharmacodynamic studies may be necessary to confirm this enhanced bioavailability in terms of improved therapeutic efficacy of the NMPs.

Stability studies

The final optimized NMPs were subjected to accelerated stability studies to determine their effectiveness upon ageing. The samples from the formulation were taken at 0 months, 3 months, and 6 months. These samples were investigated for physical appearance, drug content, micromeritic properties, and dissolution. The obtained results are shown in Table 8.

The findings from the accelerated stability studies (presented in Table 8) demonstrated that there were no significant changes observed with physical appearance, color, and texture. In addition, the micromeritic properties, such as particle size and angle repose, were found not altered. Most importantly, the results of dissolution reported as the T90% were also found to be similar before, during, and after subjecting to the accelerated storage conditions. These findings demonstrated that the optimized NMPs exhibited acceptable stability.

CONCLUSION

The process of nanocrystallization, through ultrasonication, was utilized to make INCs that exhibited increased solubility and dissolution rate of the ICZ. The solubility and dissolution of ICZ were investigated through CCD to analyze the impact of four distinct formulation and process factors. The investigation conducted through the QbD approach indicated that all the factors had a substantial effect on both the solubility and dissolution rate of the ICZ from the INCs. The optimization studies aimed at maximizing these features resulted in a formulation of INCs made using 50% amplitude for 15 min of sonication time, with 0.75% w/v of PLX-188 as the stabilizer. This formulation was determined to be the optimal formulation. Compared with the plain ICZ these optimized INCs demonstrated a 7.8-fold increase in dissolution rate. These INCs are subsequently incorporated into a lactose matrix through the process of lyophilization, resulting in the formation of NMPs. The findings from the analysis of the micromeritic properties and dissolution studies of the NMPs indicated enhanced aerodynamic and micromeritic properties, while maintaining the crystalline structure and dissolution characteristics of the INCs. The pharmacokinetic parameters derived from the lung drug levels through non-compartmental analysis indicate that the initial drug levels from the inhalational NMPs were significantly elevated in comparison to those from the oral marketed product. The $AUC_{0-\infty}$ of ICZ in the lungs through the inhalational route was determined to be 3144.97 h. µg/mL, representing a 49.9-fold increase compared to the oral marketed product, which measured 63.01 h. µg/mL. The collective findings indicate that the NMPs exhibited remarkable efficacy in administering substantially greater quantities of drug to the lungs, while also sustaining effective drug concentrations in the pulmonary region for an extended duration, in contrast to the traditional oral administration method. Therefore, these NMPs are appropriate for being administration through inhalation into the lungs, successfully accomplishing the objectives of the study.

ACKNOWLEDGMENT

Authors would like to acknowledge the higher authorities of SPMVV, Tirupati, and Hindu College of Pharmacy, Guntur, for providing facilities to run the research work smoothly.

FUNDING

No funding was received to carry out this work.

AUTHORS CONTRIBUTIONS

Yallamalli IM contributed in the research idea and work plan. SP contributed in the execution of the work, obtaining the data and drafting the manuscript. Yallamilli IM contributed in the final review of the manuscript.

CONFLICTS OF INTERESTS

The authors declare no conflicts.

REFERENCES

1. Kanaujia R, Singh S, Rudramurthy SM. Aspergillosis: An update on clinical spectrum, diagnostic schemes, and management. Curr Fungal Infect Rep. 2023:1-12. doi: 10.1007/s12281-023-00461-5, PMID 37360858
2. Arastehfar A, Carvalho A, Houbraken J, Lombardi L, Garcia-Rubio R, Jenks JD, *et al*. *Aspergillus fumigatus* and aspergillosis: From basics to clinics. Stud Mycol. 2021;100:100115. doi: 10.1016/j.simyco.2021.100115, PMID 34035866
3. Swaminathan S, Sangwai M, Wawdhane S, Vavia P. Soluble itraconazole in tablet form using disordered drug delivery approach: Critical scale-up considerations and bioequivalence studies. AAPS PharmSciTech. 2013;14(1):360-74. doi: 10.1208/s12249-012-9918-9, PMID 23334999
4. Abuhelwa AY, Foster DJ, Mudge S, Hayes D, Upton RN. Population pharmacokinetic modeling of itraconazole and hydroxyitraconazole for oral SUBA-itraconazole and sporanox capsule formulations in healthy subjects in fed and fasted states. Antimicrob Agents Chemother. 2015;59(9):5681-96. doi: 10.1128/AAC.00973-15, PMID 26149987
5. Darwich M, Mohylyuk V, Kolter K, Bodmeier R, Dashevskiy A. Enhancement of itraconazole solubility and release by hot-melt extrusion with soluplus®. J Drug Deliv Sci Technol. 2023;81:104280. doi: 10.1016/j.jddst.2023.104280
6. Lee JH, Park C, Weon KY, Kang CY, Lee BJ, Park JB. Improved bioavailability of poorly water-soluble drug by targeting increased absorption through solubility enhancement and precipitation inhibition. Pharmaceuticals (Basel). 2021;14(12):1255. doi: 10.3390/ph14121255, PMID 34959655
7. Devara R, Habibuddin M, Aukunuru J. Enhancement of dissolution rate of poorly soluble drug itraconazole by nanosuspension technology: Its preparation and evaluation studies. Asian J Pharm Clin Res. 2018;11(4):414-21. doi: 10.22159/ajpcr.2018.v11i4.19933
8. Newman SP. Drug delivery to the lungs: Challenges and opportunities. Ther Deliv. 2017;8(8):647-61. doi: 10.4155/tde-2017-0037, PMID 28730933
9. Labiris NR, Dolovich MB. Pulmonary drug delivery. Part I: Physiological factors affecting therapeutic effectiveness of aerosolized medications. Br J Clin Pharmacol. 2003;56(6):588-99. doi: 10.1046/j.1365-2125.2003.01892.x, PMID 14616418
10. Patil JS, Sarasija S. Pulmonary drug delivery strategies: A concise, systematic review. Lung India. 2012;29(1):44-9. doi: 10.4103/0970-2113.92361, PMID 22345913
11. Huang Z, Kłodzińska SN, Wan F, Nielsen HM. Nanoparticle-mediated pulmonary drug delivery: State of the art towards efficient treatment of recalcitrant respiratory tract bacterial infections. Drug Deliv Transl Res. 2021;11(4):1634-54. doi: 10.1007/s13346-021-00954-1, PMID 33694082
12. Plaunt AJ, Nguyen TL, Corboz MR, Malinin VS, Cipolla DC. Strategies to overcome biological barriers associated with pulmonary drug delivery. Pharmaceutics. 2022;14(2):302. doi: 10.3390/pharmaceutics14020302, PMID 35214039
13. Liang W, Pan HW, Vllasaliu D, Lam JK. Pulmonary delivery of biological drugs. Pharmaceutics. 2020;12(11):1025. doi: 10.3390/

pharmaceutics12111025, PMID 33114726
14. Ruge CA, Kirch J, Lehr CM. Pulmonary drug delivery: From generating aerosols to overcoming biological barriers-therapeutic possibilities and technological challenges. Lancet Respir Med. 2013;1(5):402-13. doi: 10.1016/S2213-2600(13)70072-9, PMID 24429205
15. Geiser M. Update on macrophage clearance of inhaled micro- and nanoparticles. J Aerosol Med Pulm Drug Deliv. 2010;23(4):207-17. doi: 10.1089/jamp.2009.0797, PMID 20109124
16. Gustafson HH, Holt-Casper D, Grainger DW, Ghandehari H. Nanoparticle uptake: The phagocyte problem. Nano Today. 2015;10(4):487-510. doi: 10.1016/j.nantod.2015.06.006, PMID 26640510
17. Kim S, Choi IH. Phagocytosis and endocytosis of silver nanoparticles induce interleukin-8 production in human macrophages. Yonsei Med J. 2012;53(3):654-7. doi: 10.3349/ymj.2012.53.3.654, PMID 22477013
18. Yue P, Zhou W, Huang G, Lei F, Chen Y, Ma Z, *et al*. Nanocrystals based pulmonary inhalation delivery system: Advance and challenge. Drug Deliv. 2022;29(1):637-51. doi: 10.1080/10717544.2022.2039809, PMID 35188021
19. Sabourian P, Yazdani G, Ashraf SS, Frounchi M, Mashayekhan S, Kiani S, *et al*. Effect of physico-chemical properties of nanoparticles on their intracellular uptake. Int J Mol Sci. 2020;21(21):8019. doi: 10.3390/ijms21218019, PMID 33126533
20. Qie Y, Yuan H, Von Roemeling CA, Chen Y, Liu X, Shih KD, *et al*. Surface modification of nanoparticles enables selective evasion of phagocytic clearance by distinct macrophage phenotypes. Sci Rep. 2016;6:26269. doi: 10.1038/srep26269, PMID 27197045
21. Augustine R, Hasan A, Primavera R, Wilson RJ, Thakor AS, Kevadiya BD. Cellular uptake and retention of nanoparticles: Insights on particle properties and interaction with cellular components. Mater Today Commun. 2020;25:101692. doi: 10.1016/j.mtcomm.2020.101692
22. Brunet K, Martellosio JP, Tewes F, Marchand S, Rammaert B. Inhaled antifungal agents for treatment and prophylaxis of bronchopulmonary invasive mold infections. Pharmaceutics. 2022;14(3):641. doi: 10.3390/pharmaceutics14030641, PMID 35336015
23. Demoly P, Hagedoorn P, De Boer AH, Frijlink HW. The clinical relevance of dry powder inhaler performance for drug delivery. Respir Med. 2014;108(8):1195-203. doi: 10.1016/j.rmed.2014.05.009, PMID 24929253
24. Paranjpe M, Müller-Goymann CC. Nanoparticle-mediated pulmonary drug delivery: A review. Int J Mol Sci. 2014;15(4):5852-73. doi: 10.3390/ijms15045852, PMID 24717409
25. Liu T, Han M, Tian F, Cun D, Rantanen J, Yang M. Budesonide nanocrystal-loaded hyaluronic acid microparticles for inhalation: *In vitro* and *in vivo* evaluation. Carbohydr Polym. 2018;181:1143-52. doi: 10.1016/j.carbpol.2017.11.018, PMID 29253943
26. Chakravarthy PS, Grandhi S, Swami R, Singh I. Quality by design based optimization and development of cyclodextrin inclusion complexes of quercetin for solubility enhancement. Biointerface Res Appl Chem. 2023;13(5):424. doi: 10.33263/briac135.424
27. Baldassarre F, Tatulli G, Vergaro V, Mariano S, Scala V, Nobile C, *et al*. Sonication-assisted production of fosetyl-al nanocrystals: Investigation of human toxicity and *in vitro* antibacterial efficacy against *Xylella fastidiosa*. Nanomaterials (Basel). 2020;10(6):1174. doi: 10.3390/nano10061174, PMID 32560195
28. Haiss MA, Maraie NK. Utilization of ultrasonication technique for the preparation of apigenin nanocrystals. Int J Drug Deliv Technol. 2021;11:964-73.
29. Lucero-Borja D, Subirats X, Barbas R, Prohens R, Avdeef A, Ràfols C. Potentiometric CheqSol and standardized shake-flask solubility methods are complimentary tools in physicochemical profiling. Eur J Pharm Sci. 2020;148:105305. doi: 10.1016/j.ejps.2020.105305, PMID 32184154
30. Veseli A, Žakelj S, Kristl A. A review of methods for solubility determination in biopharmaceutical drug characterization. Drug Dev Ind Pharm. 2019;45(11):1717-24. doi: 10.1080/03639045.2019.1665062, PMID 31512934
31. Srikar G, Rani AP. Tenofovir loaded poly (lactide-co-glycolide) nanocapsules: Formulation optimization by desirability functions approach. Indian J Pharm Educ Res. 2020;54(2s):S230-40. doi: 10.5530/ijper.54.2s.79
32. Srikar G, Rani AP. Study on influence of polymer and surfactant on in vitro performance of biodegradable aqueous-core nanocapsules of tenofovirdisoproxil fumarate by response surface methodology. Braz J Pharm Sci. 2019;55:e18736. doi: 10.1590/s2175-97902019000118736
33. Jia Z, Li J, Gao L, Yang D, Kanaev A. Dynamic light scattering: A powerful tool for *in situ* nanoparticle sizing. Colloids Interfaces. 2023;7(1):15. doi: 10.3390/colloids7010015
34. Bohr A, Water J, Beck-Broichsitter M, Yang M. Nanoembedded microparticles for stabilization and delivery of drug-loaded nanoparticles. Curr Pharm Des. 2015;21(40):5829-44. doi: 10.2174/1381612821666151008124322, PMID 26446473
35. Mohammadpour F, Kamali H, Hadizadeh F, Bagheri M, Shiadeh SN, Nazari A, *et al*. The PLGA microspheres synthesized by a thermosensitive hydrogel emulsifier for sustained release of risperidone. J Pharm Innov. 2022;17(3):712-24. doi: 10.1007/s12247-021-09544-7
36. Janoszka N, Azhdari S, Hils C, Coban D, Schmalz H, Gröschel AH. Morphology and degradation of multicompartment microparticles based on semi-crystalline polystyrene-block-polybutadiene-block-poly(L-lactide) triblock terpolymers. Polymers (Basel). 2021;13(24):4358. doi: 10.3390/polym13244358, PMID 34960909
37. Maheshwari R, Todke P, Kuche K, Raval N, Tekade RK. Micromeritics in pharmaceutical product development. In: Tekade RK, editor. Dosage form design considerations. 1st ed. Cambridge: Academic Press; 2018. p. 599-635. doi: 10.1016/B978-0-12-814423-7.00017-4
38. Miyamoto K, Taga H, Akita T, Yamashita C. Simple method to measure the aerodynamic size distribution of porous particles generated on lyophilizate for dry powder inhalation. Pharmaceutics. 2020;12(10):976. doi: 10.3390/pharmaceutics12100976, PMID 33076510
39. Tansho S, Abe S, Ishibashi H, Torii S, Otani H, Ono Y, *et al*. Efficacy of intravenous itraconazole against invasive pulmonary aspergillosis in neutropenic mice. J Infect Chemother. 2006;12(6):355-62. doi: 10.1007/s10156-006-0479-2, PMID 17235640
40. Kaur J, Muttil P, Verma RK, Kumar K, Yadav AB, Sharma R, *et al*. A hand-held apparatus for "nose-only" exposure of mice to inhalable microparticles as a dry powder inhalation targeting lung and airway macrophages. Eur J Pharm Sci. 2008;34(1):56-65. doi: 10.1016/j.ejps.2008.02.008, PMID 18387284
41. Compas D, Touw DJ, De Goede PN. Rapid method for the analysis of itraconazole and hydroxyitraconazole in serum by high-performance liquid chromatography. J Chromatogr B Biomed Appl. 1996;687(2):453-6. doi: 10.1016/s0378-4347(96)00245-9, PMID 9017471
42. Zhang Y, Huo M, Zhou J, Xie S. PKSolver: An add-in program for pharmacokinetic and pharmacodynamic data analysis in Microsoft excel. Comput Methods Programs Biomed. 2010;99(3):306-14. doi: 10.1016/j.cmpb.2010.01.007, PMID 20176408
43. Jacob S, Nair AB, Shah J. Emerging role of nanosuspensions in drug delivery systems. Biomater Res. 2020;24:3. doi: 10.1186/s40824-020-0184-8, PMID 31969986
44. Gagliardi A, Voci S, Salvatici MC, Fresta M, Cosco D. Brij-stabilized zein nanoparticles as potential drug carriers. Colloids Surf B Biointerfaces. 2021;201:111647. doi: 10.1016/j.colsurfb.2021.111647, PMID 33639515
45. Lotfy NS, Borg TM, Mohamed EA. The promising role of chitosan-Poloxamer 188 nanocrystals in improving diosmin dissolution and therapeutic efficacy against ferrous sulfate-induced hepatic injury in rats. Pharmaceutics. 2021;13(12):2087. doi: 10.3390/pharmaceutics13122087, PMID 34959367
46. Srikar G, Avula P, Annapurna S, Boola M. Development of extended release matrix tablets of felodipine through solid dispersions for better drug release profile by a 3^2 factorial design. Indian J Pharm Educ Res. 2016;50:S89-99.
47. Ruiz E, Orozco VH, Hoyos LM, Giraldo LF. Study of sonication parameters on PLA nanoparticles preparation by simple emulsion-evaporation solvent technique. Eur Polym J. 2022;173:111307. doi: 10.1016/j.eurpolymj.2022.111307
48. Zhang T, Li X, Xu J, Shao J, Ding M, Shi S. Preparation, characterization, and evaluation of breviscapine nanosuspension and its freeze-dried powder. Pharmaceutics. 2022;14(5):923. doi: 10.3390/pharmaceutics14050923, PMID 35631508
49. Gigliobianco MR, Casadidio C, Censi R, Di Martino P. Nanocrystals of poorly soluble drugs: drug bioavailability and physicochemical stability. Pharmaceutics. 2018;10(3):134. doi: 10.3390/pharmaceutics10030134, PMID 30134537
50. Gulsun TU, Akdag YA, Izat N, Oner L. Sahin S. Effect of particle size and surfactant on the solubility, permeability and dissolution characteristics of deferasirox. J Res Pharm 2019;23:851-9.
51. Dos Santos AM, Meneguin AB, Fonseca-Santos B, Chaves de Souza MP, Barboza Ferreira LM, Sábio RM, *et al.* The role of stabilizers and mechanical processes on physico-chemical and anti-inflammatory properties of methotrexate nanosuspensions. J Drug Deliv Sci Technol. 2020;57:101638. doi: 10.1016/j.jddst.2020.101638
52. Smail SS, Ghareeb MM, Omer HK, Al-Kinani AA, Alany RG. Studies on surfactants, cosurfactants, and oils for prospective use in formulation of ketorolac tromethamine ophthalmic nanoemulsions.

Pharmaceutics. 2021;13(4):467. doi: 10.3390/pharmaceutics13040467, PMID 33808316

53. Sandhya M, Ramasamy D, Sudhakar K, Kadirgama K, Harun WS. Ultrasonication an intensifying tool for preparation of stable nanofluids and study the time influence on distinct properties of graphene nanofluids - a systematic overview. Ultrason Sonochem. 2021;73:105479. doi: 10.1016/j.ultsonch.2021.105479, PMID 33578278
54. Bolourchian N, Shafiee Panah M. The effect of surfactant type and concentration on physicochemical properties of carvedilol solid dispersions prepared by wet milling method. Iran J Pharm Res. 2022;21(1):e126913. doi: 10.5812/ijpr-126913, PMID 36060905
55. Gaul R, Ramsey JM, Heise A, Cryan SA, Greene CM. Nanotechnology approaches to pulmonary drug delivery. In: Grumezescu AM, editor. Design of Nanostructures for Versatile Therapeutic Applications. 1st ed. New York: William Andrew Publishing; 2018. p. 221-53. doi: 10.1016/B978-0-12-813667-6.00006-1
56. Chan HW, Chow S, Zhang X, Zhao Y, Tong HH, Chow SF. Inhalable nanoparticle-based dry powder formulations for respiratory diseases: Challenges and strategies for translational research. AAPS PharmSciTech. 2023;24(4):98. doi: 10.1208/s12249-023-02559-y, PMID 37016029
57. Hebbink GA, Jaspers M, Peters HJ, Dickhoff BH. Recent developments in lactose blend formulations for carrier-based dry powder inhalation. Adv Drug Deliv Rev. 2022;189:114527. doi: 10.1016/j.addr.2022.114527, PMID 36070848
58. Li M, Lopez N, Bilgili E. A study of the impact of polymer-surfactant in drug nanoparticle coated pharmatose composites on dissolution performance. Adv Powder Technol. 2016;27(4):1625-36. doi: 10.1016/j.apt.2016.05.026
59. Shin JH, Choi KY, Kim YC, Lee MG. Dose-dependent pharmacokinetics of itraconazole after intravenous or oral administration to rats: Intestinal first-pass effect. Antimicrob Agents Chemother. 2004;48(5):1756-62. doi: 10.1128/AAC.48.5.1756-1762.2004, PMID 15105131
60. Buil JB, Hagen F, Chowdhary A, Verweij PE, Meis JF. Itraconazole, voriconazole, and posaconazole CLSI MIC distributions for wild-type and azole-resistant *Aspergillus fumigatus* isolates. J Fungi (Basel). 2018;4(3):103. doi: 10.3390/jof4030103, PMID 30158470